

Structure and self-similarity of silica aerogels

René Vacher, Thierry Woignier, and Jacques Pelous

*Laboratoire de Science des Matériaux Vitreux, Université des Sciences et Techniques du Languedoc,
F-34060 Montpellier, France*

Eric Courtens

IBM Research Division, Zurich Research Laboratory, 8803 Rüschlikon, Switzerland

(Received 26 May 1987; revised manuscript received 15 October 1987)

Small-angle neutron scattering from silica aerogels reveals that they form *mutually* self-similar volume fractals for a wide range of densities and preparations. The fractal dimension is $D = 2.40 \pm 0.03$. The fractal behavior extends down to near-molecular sizes. Indication for a volume-to-surface fractal crossover is also obtained. These results apply to neutrally prepared or acid-catalyzed materials. Base-catalyzed gels have widely different properties.

It is generally accepted that silica gels form fractal structures.^{1,2} Volume fractals are observed over intermediate sizes L , smaller than a correlation length ξ , and larger than a mean-particle diameter a , $\xi > L > a$.^{1,3} Here, the term "particles" is used to designate the homogeneous microclusters. For silica gels, the size and number of those particles, as well as their spatial arrangements, depend on the pH during reaction.⁴ It is so far not known whether materials of different macroscopic densities can be prepared which exhibit the same self-similar structure in the fractal region. In this report, we present results of a small-angle neutron-scattering (SANS) investigation performed on a series of silica aerogels of various densities and preparation conditions.⁵ We find that neutrally reacted gels have *mutually* self-similar fractal structures over a broad range of macroscopic densities ρ , and that the lighter gels are fractal over at least 2 orders of magnitude in L , down to near-molecular dimensions. For the particles, we have indications for a density-, and pH-dependent crossover from a volume to a surface fractal. Their roughness can be smoothed by oxidation. Our findings form a necessary basis for the interpretation of scaling analyses involving different materials.⁶ They reveal an important aspect of structures obtained by cluster-cluster aggregation (CCA).^{7,8}

The alcogels were prepared by reaction of tetramethoxysilane with water in a molar ratio of 1:4 diluted by various amounts of methanol.⁵ The initial pH was adjusted by addition of HCl or NH₄OH. After long aging at 55 °C, the gels were hypercritically dried.⁵ The density was determined by weighing. SANS was performed at the Laboratoire Léon Brillouin (LLB) in Saclay, France, on the PACE spectrometer.⁹ The experiment was performed with neutron wavelengths of $\lambda = 5.55, 12.3, \text{ and } 22.7 \text{ \AA}$, and sample-to-detector distances of 1.2, 3.0, and 4.5 m, respectively. The corresponding scattering vectors q range from ~ 0.0018 to $\sim 0.3 \text{ \AA}^{-1}$. The samples, in the form of $\sim 2\text{-mm}$ slices, were maintained at $\sim 70 \text{ }^\circ\text{C}$ in air, to avoid moisture. The scattered intensities $I(q)$ were corrected for transmission, for scattering of the sample cell, and for a small constant

instrumental background. $I(q)$ was normalized to the sample thickness and to incoherent scattering from a water standard.

Results obtained on gels reacted in neutral solutions are shown in Fig. 1. At intermediate q 's, one recognizes a typical power-law decrease characteristic of fractal structures.¹⁰ It saturates towards small q 's owing to the finite correlation range of the fractals. At high q 's, the departure from the power law, which is slight on the scale of Fig. 1, increases with ρ . It cannot be simply related to a trivial form factor of the particles,^{10,11} as discussed further below. The analysis first concentrates on the low- and medium- q regions (up to $q \sim 0.15 \text{ \AA}^{-1}$) which, for coherent scattering, can be fitted with¹⁰

$$I(q) = A \rho^2 \xi^3 \frac{\Gamma(D+1)}{(1+q^2 \xi^2)^{(D-1)/2}} \frac{\sin[(D-1)\arctan(q\xi)]}{(D-1)q\xi}, \quad (1)$$

where $\Gamma(x)$ is the gamma function. This expression describes both the Guinier and fractal regimes, and the crossover between those regimes. The constant A is proportional to the square of the average scattering length,¹¹ and is independent of the mean particle size a and density ρ_a for a scaling fractal for which

$$(\rho/\rho_a) = (\xi/a)^{D-3}. \quad (2)$$

The lines in Fig. 1 illustrate the excellent fits obtained with (1) up to $q \sim 0.15 \text{ \AA}^{-1}$. The corresponding values of D , ξ , and $I(q=0)$ are presented in Fig. 2. One notes that the lightest samples are fractal over about 2 orders of magnitude in q , and at least up to $q \sim 0.25 \text{ \AA}^{-1}$, corresponding to a gyration radius¹² of $\sim 4 \text{ \AA}$, a near-molecular dimension. In Fig. 2(a), one sees that $D = 2.40 \pm 0.01$ is the same for all samples, within the accuracy.

That each sample has the same D implies that a plot of local densities¹³ ρ_L versus L of different samples consists of segments of parallel lines (as shown in the inset of Fig. 4) with $\rho_L \propto L^{D-3}$ for $a \leq L \leq \xi$, and with $\rho_L = \rho_\xi = \rho$ for $L \geq \xi$, while $\rho_L = \rho_a$ for $L \leq a$. If $\rho_\xi \propto \xi^{D-3}$, with the

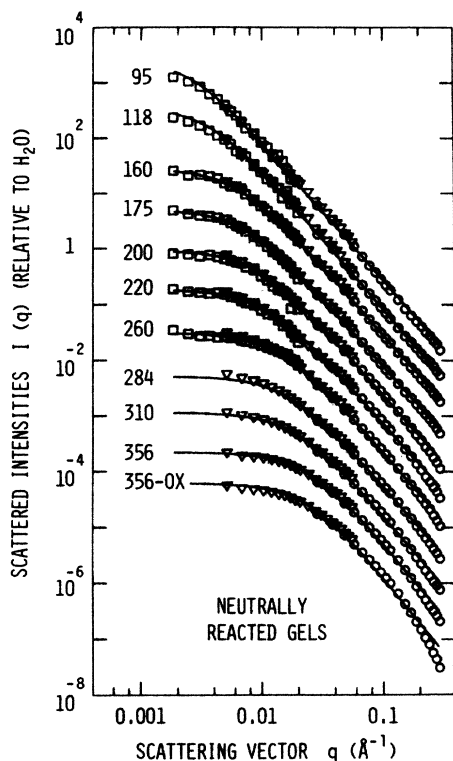


FIG. 1. Scattered intensities for 11 samples. From top to bottom: ten untreated, neutrally reacted samples of increasing density, and one oxidized sample. The curves are labeled with ρ in kg/m^3 . The different symbols refer to the three positions of the detector (see text). Measurements at a 4.5 m distance for the densest samples are not shown, as sufficient statistics were not obtained within the time available. For this figure, each intensity was divided by four compared to the previous one, starting from the top, to separate the curves. Points from only 20 out of 30 detectors are shown to improve visibility. All measured points in the range of applicability of Eq. (1) were used to fit. The solid lines correspond to Eq. (1) for the parameters shown in Fig. 2.

same D , the dotted line in the inset must collapse with all solid lines in the fractal region, revealing that all samples are *mutually* self-similar. This means that at scales L in the fractal range, different samples are then indistinguishable. From Fig. 2(b), one finds $\xi \propto \rho^{-1.67 \pm 0.05}$, giving $D = 2.40 \pm 0.02$, a value equal to that determined from Fig. 2(a), establishing the mutual self-similarity. From (2), this result is equivalent to stating that $\rho_a a^{3-D}$ is the same for all samples.

The mutual self-similarity also requires scaling of the intensities. As

$$I(0) \propto \rho^2 \xi^3 = \rho^{(3-2D)/(3-D)} (\rho_a a^{3-D})^{3/(3-D)},$$

a fit of Fig. 2(c) to a power law provides a sensitive independent verification of self-similarity. From the slope, one finds $(2D-3)/(3-D) = 3.05 \pm 0.14$, or $D = 2.41 \pm 0.02$, in remarkable agreement with the above. It can be noted that a Guinier analysis¹² of the low- q region gives essentially the same exponents for ξ and $I(0)$, with

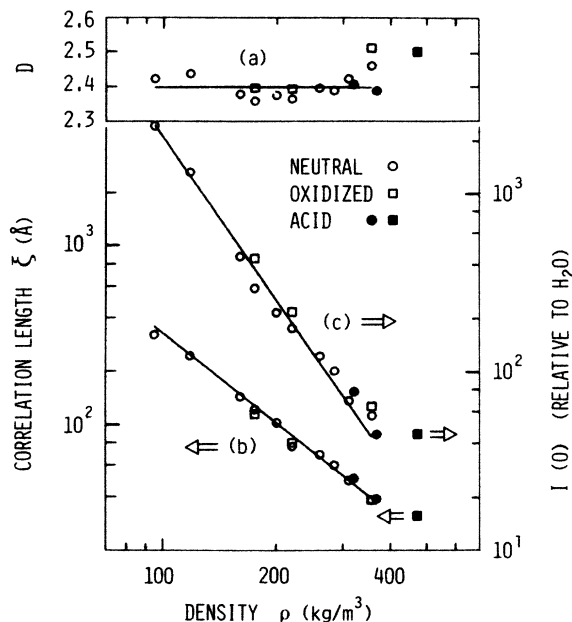


FIG. 2. The parameters obtained in fitting Eq. (1) to $I(q)$: (a) the fractal dimension D , (b) the correlation length ξ , (c) the intensity $I(0)$. The open dots are results for the ten neutral samples of Fig. 1. The solid lines are power-law fits to these values as discussed in the text. The open squares are results for three oxidized neutral samples. The solid circles are values for the two acid-catalyzed samples of Fig. 4. The solid squares are for an acid-catalyzed sample at $\text{pH}=2.5$ which departs somewhat from the general behavior.

somewhat worse accuracy. Summarizing these results, we conclude that $D = 2.40 \pm 0.03$ agrees with all the data of Fig. 1. This value also agrees with our previous determination based on the curvature of acoustic dispersion curves.⁶

To discuss the large- q behavior, we first consider the effect of oxidation in air at 500°C for 24 h. This removes residual CH_3 groups, creating new —Si—O—Si— bonds. As illustrated in Fig. 1, it does not modify $I(q)$ in the fractal and small- q regions. The values of D , ξ , and $I(0)$ for three oxidized samples (OS), also shown in Fig. 2, are seen to be near those of untreated samples (US). However, at high q , the fall of $I(q)$ with increasing q is much more rapid for OS than for US, as seen in Fig. 1, and in more detail in Fig. 3. The maximum of $q^3 I(q)$ around $q = 0.15 \text{ \AA}^{-1}$ marks the crossover from $q^3 I(q) \propto q^{3-D}$ ($D < 3$) to $q^3 I(q) \propto q^{3-\delta}$ ($\delta > 3$). The behavior of the OS is compatible with $\delta = 4$, as shown by the straight lines in Fig. 3. $I \propto q^{-4}$ is the Porod law for scattering by the smooth surface of dense particles.¹² The corresponding gyration radius is $\sim 6 \text{ \AA}$. Considering US, in Fig. 3 one notices a crossover at about the same q , with δ nearer to 3. It is thus natural to interpret this δ as a property of the particle surfaces that would thus be fractal, with a dimension $D_s \simeq 6 - \delta$.¹⁴ We find $D_s \simeq 3$ and 2.9 for $\rho = 220$ and 356, respectively, indicating very rough surfaces. The smaller the density, the higher is D_s . Oxidation smooths the surface of the particles, approximately main-

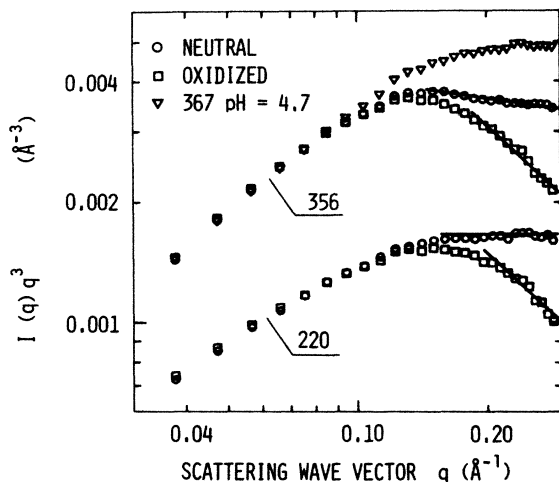


FIG. 3. Scattered intensities ($\times q^3$) for two densities in the volume-to-surface crossover region. The circles correspond to the untreated neutral samples. The squares correspond to the same material after oxidation. The triangles refer to an acid-catalyzed sample at $\text{pH}=4.7$. The lines at large q illustrate the various values of $3-\delta$ (see text). The relative shift of the curves for the different densities is the experimental one, and is in accordance with Eq. (1).

taining their mean dimension.

Figure 4 illustrates the effect of varying pH during reaction. Moderately acidic catalysis does not affect the self-similarity. Fits such as those in Fig. 4 lead to values of D , ξ , and $I(0)$ also shown in Fig. 2. Acid catalysis produces a high number of small particles.⁴ However, in the fractal region, where the structure is presumably controlled by CCA, the materials remain mutually self-similar as demonstrated by the data points of Fig. 2. For identical densities, the volume-to-surface crossover occurs at higher values of q with decreasing pH , as illustrated for one particular case in Fig. 3. This confirms that acid catalysis favors a smaller dimension a , and thus a higher density ρ_a . Figure 3 also suggests that the particle surface is fuzzier in that case. For strongly acidic catalysis, where the reaction mechanisms are different,⁴ mutual self-similarity seems to break down, as illustrated in Fig. 2 for $\text{pH}=2.5$.

Base catalysis produces relatively large particles,⁴ with a more extended Porod region (Fig. 4). The smaller number of particles corresponds to another CCA regime in which ramified structures form over a smaller range of L . The slope $-D$ in Fig. 4 is -1.9 , in agreement with CCA values at low densities.¹⁵ Even for lighter materials, the range of the fractal region in base-catalyzed samples never reaches 1 order of magnitude in L .¹ The falloff of $I(q)$ at smaller q 's suggests a correlation between gelling clusters. At the highest q 's, departure from the Porod law in the form of an overintensity is observed. This is the only region affected by oxidation, which strongly reduces that

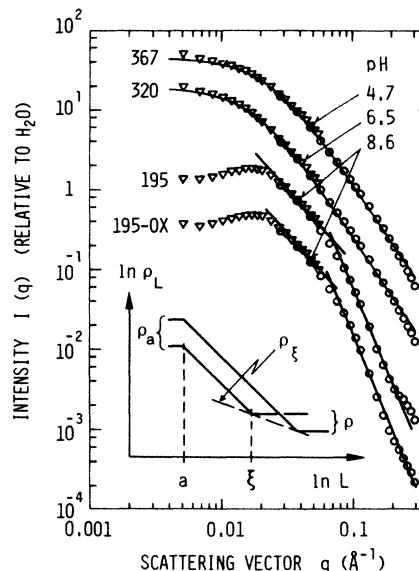


FIG. 4. Scattered intensities for four samples. From top to bottom: acid catalyzed at $\text{pH}=4.7$ and 6.5 with fits to Eq. (1); base-catalyzed at $\text{pH}=8.6$, and the latter oxidized. Symbols and relative shifts of the curves as in Fig. 1. The straight lines on the lower two curves correspond to $D=1.9$ for small q , and $\delta=4$ for large q . The inset is discussed in the text.

feature.

In summary, we have shown that CCA with a high density of particles forms mutually self-similar structures over a surprisingly broad range of preparation conditions, with a fractal dimension $D=2.40\pm 0.03$. This value is somewhat smaller than the $D\approx 2.5$ of the infinite cluster of a percolating network.¹⁶ The small difference with the latter could possibly be accounted for by some polydispersity.¹⁷ Interestingly, *mutual* self-similarity seems to occur in other systems as well,¹⁸ although we appear to be first in introducing the concept. It is a necessary property for the scaling of data obtained on different gels.⁶ It should be noted that a series of Brillouin measurements performed on the materials used here does scale with $D=2.40$, and a fracton dimension of 1.25 ± 0.1 , in perfect agreement with Ref. 6. This will be reported in detail elsewhere. Finally, our observations also reveal that different gels can be *dissimilar* at the size of the constituent particles. The latter are rather sensitive to the preparation conditions, with a surface-fractal microstructure which can also be modified by oxidation. This can affect the scaling of particle-dependent properties.

Appreciation is expressed to the LLB for the use of its experimental facilities and to Dr. J. Teixeira for his invaluable collaboration during measurements. We also thank Dr. J. Phalippou for useful discussions. The LLB is a Laboratoire Commun Commissariat à l'Énergie-Centre National de la Recherche Scientifique.

- ¹D. W. Schaefer and K. D. Keefer, *Phys. Rev. Lett.* **56**, 2199 (1986).
- ²D. Rojanski, D. Huppert, H. D. Bale, Xie Dacai, P. W. Schmidt, D. Farin, A. Seri-Levy, and D. Avnir, *Phys. Rev. Lett.* **56**, 2505 (1986).
- ³Sow Hsin Chen and J. Teixeira, *Phys. Rev. Lett.* **57**, 2583 (1986).
- ⁴R. K. Iler, *The Chemistry of Silica* (Wiley, New York, 1979).
- ⁵T. Woignier, J. Phalippou, and J. Zarzycki, *J. Non-Cryst. Solids* **63**, 117 (1984). The gels were reacted and cured at 55°C, for 12–15 d. They were dried at 270°C and 180 bars, with a heating cycle of 3 h, and a drying cycle of 2 h.
- ⁶E. Courtens, J. Pelous, J. Phalippou, R. Vacher, and T. Woignier, *Phys. Rev. Lett.* **58**, 128 (1987).
- ⁷P. Meakin, *Phys. Rev. Lett.* **51**, 1119 (1983).
- ⁸M. Kolb, R. Botet, and R. Jullien, *Phys. Rev. Lett.* **51**, 1123 (1983).
- ⁹For a description of the instrument, see *Equipements Expérimentaux* (LLB, CEN-Saclay, France, 1987), pp. 131–133.
- ¹⁰S. K. Sinha, T. Freltoft, and J. Kjems, in *Kinetics of Aggregation and Gelation*, edited by F. Family and D. P. Landau (Elsevier, Amsterdam, 1984), p. 87.
- ¹¹J. Teixeira, in *On Growth and Form*, edited by H. E. Stanley and N. Ostrowsky (Nijhoff, Dordrecht, 1986), p. 145; T. Freltoft, K. J. Kjems, and S. K. Sinha, *Phys. Rev. B* **33**, 269 (1986).
- ¹²A. Guinier, *Théorie et Technique de la Radiocristallographie* (Dunod, Paris, 1956).
- ¹³A. Kapitulnik, A. Aharony, G. Deutscher, and D. Stauffer, *J. Phys. A* **16**, L269 (1983).
- ¹⁴H. D. Bale and P. W. Schmidt, *Phys. Rev. Lett.* **53**, 596 (1984).
- ¹⁵M. Kolb, R. Jullien, and R. Botet, in *Scaling Phenomena in Disordered Systems*, edited by R. Pynn and A. Skjeltorp (Plenum, New York, 1985), p. 71.
- ¹⁶D. Stauffer, in *On Growth and Form*, Ref. 11, pp. 79–100.
- ¹⁷J. E. Martin and A. J. Hurd, *J. Appl. Cryst.* **20**, 61 (1987).
- ¹⁸G. Dietler, C. Aubert, D. S. Cannell, and P. Wiltzius, *Phys. Rev. Lett.* **57**, 3117 (1986).